Published in final edited form as:
Free Radic Biol Med. 2009 July 1; 47(1): 72–78. doi:10.1016/j.freeradbiomed.2009.04.002.

Lipophilicity of potent porphyrin-based antioxidants. Comparison of *ortho* and *meta* isomers of Mn(III) *N*-alkylpyridylporphyrins

Ivan Kos[1], **Júlio S. Rebouças**[1], **Gilson DeFreitas-Silva**[1], **Daniela Salvemini**[2], **Zeljko Vujaskovic**[1], **Mark W. Dewhirst**[1], **Ivan Spasojevic**[3], and **Ines Batinic-Haberle**[1,*]

1 *Department of Radiation Oncology, University Medical School, Durham NC 27710*

3 *Department of Medicine Duke, University Medical School, Durham NC 27710*

2 *Department of Internal Medicine, Division of Pulmonary, Critical Care and Sleep Medicine, Saint Louis University, St. Louis, MO 63110, USA*

Abstract

Mn(III) *N*-alkylpyridylporphyrins are among the most potent known SOD mimics and catalytic peroxynitrite scavengers, and modulators of redox-based cellular transcriptional activity. In addition to their intrinsic antioxidant capacity, bioavailability plays major role in their *in vivo* efficacy. While of identical antioxidant capacity, lipophilic MnTnHex-2-PyP is up to 120-fold more efficient in reducing oxidative stress injuries than hydrophilic MnTE-2-PyP. Due to limitations of analytical nature, porphyrin lipophilicity has been often estimated by thin-layer chromatographic R_f parameter, instead of the standard n-octanol/water partition coefficient, P_{OW}. Herein we used a new methodological approach to finally describe the MnP lipophilicity, by the conventional log P_{OW} means, for a series of biologically active *ortho* and *meta* isomers of Mn(III) *N*-alkylpyridylporphyrins. Three new porphyrins (MnTnBu-3-PyP, MnTnHex-3-PyP and MnTnHep-2-PyP) were synthesized to strengthen the conclusions. The log P_{OW} was linearly related to R_f and to the number of carbons in the alkyl chain (nC) for both isomer series; the *meta* isomers being 10-fold more lipophilic than the analogous *ortho* porphyrins. Increasing the length of the alkyl chain for 1 carbon atom increases the log P_{OW} value ~ 1 log unit with both isomers. Dramatic ~4 and ~5 orders of magnitude increase in lipophilicity of *ortho* isomers by extending pyridyl alkyl chains from 2 (MnTE-2-PyP, log $P_{OW} = -6.25$) to 6 (MnTnHex-2-PyP, log $P_{OW} = -2.29$) and 8 carbon atoms (MnTnOct-2-PyP, log $P_{OW} = -0.77$) parallels the increased efficacy in several oxidative-stress injury models, particularly those of the central nervous system where transport across the blood-brain barrier is critical. Although *meta* isomers are only slightly less potent SOD mimics and antioxidants than their *ortho* analogues, their higher lipophilicity and smaller bulkiness may lead to a higher cellular uptake and overall similar effectiveness *in vivo*.

Introduction

Oxidative stress is a common state in most pathological conditions such as cancer, diabetes, radiation injury, disorders of central nervous system (Alzheimer's, Parkinson's, multiple

Corresponding author: Ines Batinic-Haberle, Ph. D., Department of Radiation Oncology-Cancer Biology, Duke University Medical Center, Research Drive, 281b/285 MSRB I, Box 3455, Durham, NC 27710, Tel: 919-684-2101, Fax: 919-684-8718, e-mail: E-mail: iBatinic@duke.edu.

sclerosis, amyotrophic lateral sclerosis, stroke, spinal cord injury, chronic morphine tolerance), etc [1]. Thus synthetic antioxidants such as metal complexes (Mn salens [2], Mn cyclic polyamines [3], Mn porphyrins (MnP) [4]) and nitroxides [5] have been developed. Given the key role of mitochondria, compounds that accumulate there, such as MitoQ [6,7] and Mn porphyrins [8] are of particular interest.

We have developed metalloporphyrin-based compounds that are potent mimics of superoxide dismutase based on structure-activity relationships (SAR) between the ability of MnPs to catalytically remove superoxide and the metal-centered redox potential for the $Mn^{III}P/Mn^{II}P$ redox couple, $E_{1/2}$ [9,10]. The ability of Mn porphyrins to scavenge superoxide parallels their ability to catalytically remove peroxynitrite, a more harmful and powerful oxidant *in vivo* [11]. Levels of $O_2^{\cdot-}$ and $ONOO^-$ and the other species that they generate ($OH^{\cdot}$, H_2O_2, $CO_3^{\cdot-}$, $NO_2^{\cdot}$) are increased under pathological conditions and damage biological molecules leading to their loss of function. Such species also upregulate cellular transcription, propagating oxidative stress and, thus, the related disease condition. Indeed we have found that Mn porphyrins inhibit activation of major transcription factors, AP-1 [12], NF-κB [13,14] and HIF-1α [15].

The Mn(III) *ortho meso*-tetrakis-*N*-ethylpyridylporphyrin, MnTE-2-PyP is the prototypical MnP-based SOD mimic/peroxynitrite scavenger most studied *in vivo* [16–25]. Its efficacy *in vivo* is at least in part due to its accumulation in mitochondria [8] and, despite its overall 5+ charge, its pharmacokinetics in the mouse shows that the drug distributes into major tissues and organs, including the brain [15].

The most efficacious compounds with high k_{cat}, Mn(III) *ortho meso*-tetrakis-*N*-alkylpyridylporphyrins, have positively charged groups in *ortho* positions, in close vicinity to the metal site. Such design affords thermodynamic and electrostatic facilitation for the approach of negatively charged superoxide to the Mn center [10]. Recent studies have strongly supported the assumption that, in addition to high antioxidant potency, MnP bioavailability plays a major role, particularly in central nervous system disorders [26]. A MnTE-2-PyP analogue of equivalent antioxidant potency has been designed and synthesized with longer alkyl chains to yield an *intuitively* more lipophilic derivative, i.e. MnTnHex-2-PyP (Figure 1) [9]. Indeed, we have shown that MnTnHex-2-PyP is more effective in facilitating aerobic growth of SOD-deficient *E. coli* than its ethyl analogue (due at least in part to the fact that it accumulates in *E. coli* better [27]), thus offering protection at > 2 orders of magnitude lower concentration than MnTE-2-PyP [27]. The SOD-deficient *E. coli* that grew in the presence of MnTnHex-2-PyP has significantly higher ability to dismute $O_2^{\cdot-}$ than if *E. coli* grew in the presence of MnTE-2-PyP [27]. In animal models, MnTnHex-2-PyP was up to 120-fold more effective than MnTE-2-PyP (see Discussion also) at lowest therapeutically relevant doses (0.05 mg/kg) than any synthetic antioxidant thus far reported [1–4]. In rats, MnTnHex-2-PyP distributes between blood and brain at an 8:1 ratio 30 min after iv injection, while the corresponding ratio is 100:1 with MnTE-2-PyP [13,15] [2]). In cerebral palsy model[3] preliminary data show that only MnTnHex-2-PyP, but not MnTE-2-PyP, was effective when given to pregnant rabbit dam twice (intravenously), before and after uterus ischemia at only 0.05 mg/kg (0.6 mg total dose per rabbit dam). The efficacy has been ascribed to the improved ability of MnTnHex-2-PyP to cross several lipid barriers before entering fetal brain [3]. While both MnTE-2-PyP and MnTnHex-2-PyP are promising for clinical development, the latter is advantageous for central nervous system (CNS) injuries due to its higher ability to cross the blood-brain barrier. To note, both MnTE-2-PyP and MnTnHex-2-PyP are extremely stable and do not lose redox-active Mn site in the presence of other ligands (EDTA). No loss of MnTnHex-2-PyP happens within 3 months in 12 M HCl and only 50% of MnTE-2-PyP was lost within a month [9].

Whereas the lipophilicity of MnPs seems to be a critical parameter for their action *in vivo*, it is often estimated in terms of the thin-layer chromatographic (TLC) retention factor values (R_f), which is not a common pharmaceutical parameter of drug lipophilicity and is meaningless for medical and pharmaceutical audiences, as it precludes the comparison with other drugs targeting similar diseases. A more familiar lipophilicity descriptor is the n-octanol/water partition coefficients (P_{OW}). However, MnPs distribute into n-octanol at extremely low levels, which imposes difficulties of analytical nature in determining log P_{OW}. Herein we have adapted a recent strategy [28] to determine the log P_{OW} of *ortho* and *meta* isomeric Mn porphyrins, and show that actual log P_{OW}, whose measurements are cumbersome, can be quickly and easily predicted based upon simple and straightforward R_f determinations.

Methods

General

Xanthine and equine ferricytochrome *c* (lot no. 7752) were from Sigma, whereas xanthine oxidase was prepared by R. Wiley [29] and was a gift from K.V. Rajagopalan. $MnCl_2{\cdot}4H_2O$ was purchased from J. T. Baker. Anhydrous *N*,*N*-dimethylformamide (DMF, Sigma-Aldrich Chemical Co) was kept over 4 Å molecular sieves. Ethyl ether (anhydrous), acetone, chloroform, and aluminum-backed silica gel 60 F254 TLC sheets were from EMD. NH_4PF_6 (>99.9999% purity) was from Advance Research Chemicals, Inc. KNO_3 and methanol were from Mallinckrodt. Acetonitrile was from Fisher Scientific. Plastic-backed silica gel TLC plates (Z122777-25EA, Batch#3110), tetrabutylammonium chloride and ethyl *p*-toluenesulfonate were purchased from Sigma-Aldrich. The n-butyl, n-heptyl and n-hexyl esters of *p*-toluenesulfonic acid were purchased from TCI America. All other chemicals and solvents were of analytical grade and used without further purification.

Electrospray ionization mass spectrometric analyses (ESI-MS) were performed as described elsewhere [30] on an Applied Biosystems MDS Sciex 3200 Q Trap LC/MS/MS spectrometer at Duke Comprehensive Cancer Center, Shared Resource PK Labs; all samples of ~5 μM concentration were prepared in a H_2O-acetonitrile (1:1, v/v; containing 0.1 % v/v HFBA) mixture and infused for 1 min at 10 μL/min into the spectrometer (curtain gas = 20 V; ion spray voltage = 3500 V; ion source = 30 V; T = 300 °C; declustering potential = 20 V; entrance potential = 1 V; collision energy = 5 V; gas = N_2).

UV/vis spectra were recorded in H_2O at room temperature on a Shimadzu UV-2501PC spectrophotometer with 0.5 nm resolution.

Elemental analyses were done by Atlantic MicroLab, Norcross, GA.

Porphyins

Caution needs to be exercised with all chemicals used in the synthesis including commercial porphyrins as their quality is variable [30]. The synthesis and characterization of all *ortho* isomers other than the n-heptyl analogue, which is given below, have been reported elsewhere [9]. The preparation of the other new compounds MnTnBu-3-PyP and MnTnHex-3-PyP are described below. <u>*N*-alkylation</u> . *N*-alkylation was performed as described previously [9]. Typically, to 100 mg of H_2T-2(3)-PyP (Frontier Scientific) in 20 mL DMF at 100°C was added 4 mL of the corresponding *p*-toluenesulfonate. Reaction was followed by thin-layer chromatography on silica gel TLC plates using 8:1:1 acetonitrile:KNO_3-saturated H_2O:H_2O as the mobile phase. Duration of *N*-alkylation is dependent upon the type of isomer and length of alkyl chains and ranged between few hours to few days. The course of *N*-alkylation was followed by TLC until no further change was observed. With *meta* isomers a single spot marked the completion of *N*-alkylation, while atropoisomers were observed with H_2TnHep-2-PyP.

Upon completion, the reaction mixture was poured in a separatory funnel containing 200 ml each of water and chloroform and shaken well. The chloroform layer was discarded and extraction with $CHCl_3$ was repeated several times. The aqueous layer was filtered and the porphyrin was precipitated as PF_6^- salt by dropwise addition of a concentrated aqueous solution of NH_4PF_6, until no further precipitate formed. The precipitate was filtered and thoroughly washed with diethyl ether. After air drying the precipitate was dissolved in acetone, filtered and precipitated as the chloride salt by the addition of an acetone solution of tetrabutylammonium chloride. The precipitate was washed thoroughly with acetone and dried in vacuum at room temperature. Metallation. Metallation was achieved as previously described [9]. In brief, 20-fold excess $MnCl_2$ is added to a pH 12.5 solution of porphyrins at 25 °C. Metallation occurs in a few hours at room temperature for butyl, but requires overnight heating at 100°C for the heptyl and hexyl porphyrins. The reaction progress was followed by uv/vis spectroscopy and TLC (8:1:1=acetonitrile:KNO_3-saturated H_2O:H_2O) until the disappearance of both Soret band and fluorescence of the metal-free porphyrin. Upon completion, the suspension (excess of free Mn in the form of Mn oxo/hydroxo species) was filtered off, and the filtrate was precipitated with aqueous solution of NH_4PF_6 and washed with ether. The precipitate was dissolved in acetone, precipitated with an acetone solution of tetrabuthylammonium chloride and the resulting precipitate was washed with acetone. The $PF_6^-{}_{(aq)}/Cl^-{}_{(acetone)}$ precipitation procedure was repeated twice to assure removal of free manganese.

Metal-free porphyrins and their metal complexes were characterized by thin-layer chromatography, elemental analysis, UV/vis spectroscopy and electrospray ionization mass spectrometry (ESI-MS). *UV/vis data:* the molar absorption coefficients and corresponding λ_{max} are summarized in Table 1, whereas ESI-MS data for the complexes are given in Table 2 and the peak assignments are consistent with those described for related compounds [30]. *Elemental analysis:* H_2TnBu-3-PyPCl$_4$·9H_2O. ($C_{56}H_{80}N_8O_9Cl_4$) Found: C, 58.99; H, 6.77; N, 9.88; Cl, 12.43 Calculated: C, 58.43; H, 7.00; N, 9.73; Cl, 12.31 %. H_2TnHex-3-PyPCl$_4$·13H_2O ($C_{64}H_{104}N_8O_{13}Cl_4$) Found: C, 57.49; H, 8.63; N, 8.49; Cl, 10.45 Calculated: C, 57.56; H, 7.85; N, 8.93; Cl, 10.45 %. H_2TnHep-2-PyPCl$_4$·12.5 H_2O ($C_{68}H_{111}N_8O_{12.5}Cl_4$) Found: C, 58.93; H, 7.54; N, 8.12; Cl, 10.24 Calculated: C, 59.08; H, 8.08; N, 8.11; Cl, 10.26 %. MnTnBu-3-PyPCl$_5$·14H_2O ($MnC_{56}H_{88}N_8O_{14}Cl_5$) Found: C, 50.59; H, 6.76; N, 8.45; Cl, 13.45 Calculated: C, 50.74; H, 5.85; N, 8.42; Cl, 13.33 %. MnTnHex-3-PyPCl$_5$·13H_2O Found: C, 53.80; H, 6.47; N, 7.88; Cl, 12.33 Calculated: C, 53.99; H, 7.22; N, 7.87; Cl, 12.33 %. MnTnHep-2-PyPCl$_5$·20.5H_2O ($MnC_{68}H_{125}N_8O_{20.5}Cl_5$) Found: C, 50.43; H, 6.42; N, 7.24; Cl, 9.99 Calculated: C, 50.45; H, 8.02; N, 6.82; Cl, 10.85 %.

Thin-layer chromatography

Thin-layer chromatography of the purified compounds was performed on two types of silica gel TLC plates (plastic- or aluminum-backed) with 1:1:8 KNO_3-saturated H_2O: H_2O: acetonitrile mixture as mobile phase. Typically, 1 μL of ~1 mM samples were applied at ~ 1cm of the strip border and the solvent front was allowed to run ~12 cm. The absolute R_f values and their ratio thereoff are sensitive to the degree of the saturation of vapor phase in the TLC chamber and may differ slightly from one to another experiment. Thus, the internal standardization of TLC is required for comparison purposes [30].

Partition coefficient

Partition between water and n-butanol was determined experimentally with more lipophilic *ortho* and *meta* isomeric Mn(III) *meso*-tetrakis-*N*-alkylpyridylporphyrins using a variation of the shake-flask method [28]. Briefly, 0.1 mL of a MnP solution in n-butanol-saturated water was shaken with 1 mL of water-saturated n-butanol for 3 min using Vortex-Genie in plastic tube. The biphasic mixture was centrifuged (3 min at 6000 rpm) and the layers were separated.

The concentration of the MnP in each layer was measured spectrophotometrically. If dilution was needed for the UV/vis measurements, the aqueous layer was diluted with water, whereas for the organic layer, water-saturated n-butanol was used instead. Spectrum baseline was chosen accordingly. The log P_{BW} was calculated using equation (1):

$$\log P_{BW} = \log\left(\frac{c_{nBuOH}}{c_{H2O}} \times \frac{V_{nBuOH}}{V_{H_2O}}\right) \quad (1)$$

The log P_{BW} values were converted to log P_{OW} using equation (2) as established recently [28] employing compounds that can be easily measured in both n-octanol and n-butanol (caffeine, pyridine, cyclohexanone, pyridazine, thiourea).

$$\log P_{OW} = 1.55 \cdot (\log P_{BW}) - 0.54 \quad (2)$$

The P_{OW} values for the hydrophilic members of the porphyrin series were calculated from the log P_{OW} vs R_f correlation defined in this work (see below).

SOD-like activity

Determination of the catalytic rate constant for $O_2^{\cdot -}$ dismutation using cyt *c* assay was performed as previously described in details [9].

Results

SOD-activity

All MnP studied here are good-to-potent SOD mimics. The catalytic rate constants for the dismutation of $O_2^{\cdot -}$ are given in Table 3.

Thin-layer chromatography

The R_f values measured for the compounds in silica gel plates (plastic-backed, $R_{f(Plastic)}$) are given in Table 3. A linear relationship between $R_{f(Plastic)}$ values and the corresponding values obtained using aluminum-backed plates ($R_{f(Al)}$) was obtained and is depicted in Figure 2. Our data show that both plates exhibit equally well the effect of the lengthening of the alkyl chains. Because of such a linear relationship and for convenience, all R_f vales from hereon will refer to those calculated using plastic-backed TLC plates ($R_{f(Plastic)}$).

Partition coefficients

The log P_{OW} for the MnPs are given in Table 3. Linear relationships between log P_{OW} and the number of carbon atoms in the alkyl chain were observed in the series of both isomers (Fig. 3). Of note, all *meta* isomers (eq. 3) are more lipophilic than their respective *ortho* analogues (eq. 4).

$$\log P_{OW}^{(ortho\ \text{series})} = 0.97 \cdot nC - 8.36 \quad (3)$$

$$\log P_{OW}^{(meta\ \text{series})} = 0.98 \cdot nC - 7.46 \quad (4)$$

Linear correlations between the log P_{OW} and the R_f values were also observed (Figure 4, eqs. 5 and 6). This provides an easy tool for prediction of log P_{OW} values of hydrophilic Mn porphyrins, of which direct measurement of log P_{OW} values is experimentally inaccessible. Such an approach has been used for calculating the log P_{OW} of the lower members of the *ortho* and *meta* series, including MnTE-2-PyP, as presented in Table 3.

$$\log P_{ow}^{(ortho\ \text{series})} = 12.69 \cdot R_f - 7.59 \quad (5)$$

$$\log P_{ow}^{(meta\ \text{series})} = 8.89 \cdot R_f - 6.70 \quad (6)$$

Discussion

While development of MnP-based experimental therapeutics of tailored bioavailability have been intensively pursued [26,27], limitations of analytical nature have often precluded appropriate quantification of the lipophilicity of the candidate drugs [31]. In the particular case of Mn(III) *ortho N*-alkylpyridylporphyrins, this issue has been alternatively worked around by describing the lipohilic character of the therapeutics by using their chromatographic R_f values. Such characterization of lipophilicity, while sound and relevant to chemists, is less descriptive and meaningful from a pharmaceutical/medical point of view. Partition coefficient between n-octanol and water is a common pharmaceutical measure of drug lipophilicity/bioavailability. Therefore, for a broader audience, log P_{OW} values would relate more convincingly the increase in the *in vivo* efficacy of a drug to its lipophilicity, and would also allow comparison of MnPs to other drugs of similar therapeutic use. A strategy to overcome the technical difficulties in determining P_{OW} values of compounds that do not distribute directly into the n-octanol phase at levels measurable by convenient methods (e.g., cationic MnP) may involve the use of an alternative solvent to n-octanol (such as n-butanol) and a corresponding calibration curve relating P_{OW} to the partition in the new solvent [32]. This approach was recently shown adaptable to porphyrin P_{OW} measurements [28] and was used here. The n-butanol/water distribution of the more lipophilic cationic Mn porphyrins was then measured and converted to n-octanol/water partition (eq. 2, Table 3). The P_{OW} for the hydrophilic members of the porphyrin series were calculated from the appropriate log P_{OW} vs R_f relationship (Table 3).

The log P_{OW} vs nC

Our data show that the log P_{OW} is linearly related to the number of carbon atoms in the alkyl side chain (nC) for both *ortho* and *meta* isomers. The slope of the curves is close to one in both systems, which means that each CH_2 group in the side chain contributes to an ~10-fold increase in lipophilicity. Additionally, the parallel displacement of the *meta* isomer series by 1 log unit relative to the *ortho* series indicates that the *meta* isomers are ~10-fold more lipophilic than the corresponding *ortho* species (Figs. 3 and 4). Overall, this means that *meta* compounds share the same lipophificity of the *ortho* isomers that bear alkyl chains with one more CH_2 group. Thus, the same lipophilicity of a shorter *meta* hexyl species (MnTnHex-2-PyP) was achieved with the longer *ortho* heptyl porphyrin, MnTnHep-2-PyP (Table 3).

The log P_{OW} vs R_f

We established that with both *meta* and *ortho* isomers the log P_{OW} values are linearly related to R_f values (Figure 3). It follows, thus, that both parameters are equally valid means for describing MnP lipophilicity. The linear correlation also indicates that significant differences in lipophilicity correspond with small differences in R_f values; *e.g.*, R_f changes of 0.1 for the

ortho isomers result in an ~17-fold lipophilicity increase (1.24 log P_{OW} change) (Table 3). The 0.32 difference in R_f values between *ortho* ethyl and hexyl porphyrins (MnTE-2-PyP and MnTnHex-2-PyP) yields 4 orders of magnitude difference in P_{OW} value.

As opposed to the log P_{OW} vs nC relationships, the log P_{OW} vs R_f plots of the *ortho* and *meta* series are not parallel to each other. The spatial (*ortho* vs *meta*) substitution pattern controls the overall exposure of the porphyrin core and, hence, the adsorption of the compounds onto silica gel [33]. As the core exposure in the *meta* isomers is considerably less affected by the length of the alkyl side-chain (nC) than the ortho analogues, the dependence of R_f values on nC are less pronounced in the *meta* isomers. Thus, the log P_{OW} are more responsive to R_f values in the *ortho* series than in the *meta* series, as indicated by the greater slope of eq. 5 compared to that of eq. 6).

Therapeutics that are widely used in clinics have log P values in a range from *ca* −3 to *ca* + 5 [34–36]. The members of the *ortho* series with higher lipophilicity (P_{OW} values ≥ *ca* −2) and *in vivo* efficacy, such as MnTnOct-2-PyP, MnTnHep-2-PyP, MnTnHex-2-PyP) (Table 2), may be the most promising Mn porphyrins for clinical development, particularly for CNS injuries. In five *in vivo* and *in vitro* models of oxidative stress injury MnTnHex-2-PyP proved up to 120-fold more effective than MnTE-2-PyP, offering protection at submicromolar concentrations in cell models and at only 0.05 mg/kg in animal models. In two studies (cerebral palsy and ataxia telangiectasia) the hydrophilic MnTE-2-PyP was ineffective. The models that employed MnTnHex-2-PyP are: *E. coli* [27], ataxia telangiectasia [37], kidney ischemia/reperfusion [38], chronic morphine tolerance [26], lung radioprotection [1] , stroke [2], cerebral palsy [3], amyotrophic lateral sclerosis G93A mouse model [4]. In a hippocampus organotypic slice model the octyl analogue, MnTnOct-2-PyP, was 3000-fold more protective against oxygen and glucose deprivation than the hydrophilic MnTE-2-PyP [43].

Ortho vs meta isomeric Mn(III) N-alkylpyridylporphyrins

We have previously observed that with *ortho* isomers the SOD activity (k_{cat}) drops from methyl to butyl and then increases again from butyl to octyl porphyrin [9] The data were discussed with respect to the interplay of electrostatic/steric and thermodynamic factors. However, there is essentially no difference in k_{cat} among *meta* isomers (Table 3), which is consistent with the special charge distribution/eletrostatics experienced by the Mn center in the *meta* series [40]. Consequently, as the alkyl chain grows from methyl to butyl the difference in k_{cat} between *ortho* and *meta* analogues drops from 15-fold for methyl to 3.2-fold for butyl porphyrin (Table 2), while the difference in lipophilicity remains the same (Figure 4). Further, *meta* isomers are less bulky. We have shown with methyl analogues that *meta* isomer, MnTM-3-PyP accumulates more in *E. coli* than bulkier *ortho* porphyrin MnTM-2-PyP [41]; the protection of aerobic growth of SOD-*deficient E. coli* with *ortho* and *meta* isomers was nearly identical. The unfavorable impact of bulkiness is much more pronounced with bigger molecules [27, 41,42]. Although imidazolium derivatives (MnTDE-2-ImP and MnTDMOE-2-ImP) [27,43] are equally potent SOD mimics, they accumulate less in *E. coli* and are therefore less protective than MnTE-2-PyP [27]. In summary, due to their higher lipophilicity and lesser bulkiness, *meta* porphyrins may accumulate to higher levels within a cell and that may compensate for somewhat lower k_{cat}; in turn they may be *in vivo* of similar efficacy as are *ortho* isomers (work in progress) [5].

[1]Gauter-Fleckenstein, B.; Fleckenstein, K.; Owzar, K.; Jiang, C.; Rebouças, J. S.; Batinic-Haberle, I.; Vujaskovic, Z. Early and late administration of antioxidant mimetic MnTE-2-PyP in mitigation and treatment of radiation-induced lung damage, unpublished.
[2]Sheng, H.; Spasojevic, I.; Batinic-Haberle, I.; Warner, D, unpublished.
[3]Tan, S.; Batinic-Haberle, I. The effect of MnTnHex-2-PyP in cerebral palsy rabbit model, unpublished.
[4]row, J. P.; Batinic-Haberle, I. The effect of MnTnHex-2-PyP in delaying death in G93A ALS model, unpublished.
[5]Kos, I.; Benov, L.; Spasojevic, I.; Batinic-Haberle, I. unpublished

According to Hansch et al [34] the ideal compound would have log P_{OW} = ~ 2; *ortho* Mn(III) tetrakis(*N*-undecylpyridinium-2-yl)porphyrin with log P_{OW} = 1.98 or its *meta* decyl analogue would meet such criteria. Yet, although of appropriate lipophilicity Mn(III) tetrakis(*N*-undecylpyridinium-2-yl)porphyrin is likely too big to easily accumulate within cell. As discussed above to predict the drug antioxidant efficiency *in vivo*, other parameters should be considered, particularly stericity. The size and the shape of the molecule would determine the bulkiness of the molecule, but would also affect the shielding of the positive charges; combined these effects would dominate the transport and the interactions (likely unfavorable) with biomolecules which MnP would encounters on its way through the cell. In addition to steric factors, the redox property, i.e. the reducibility of Mn^{+3} porphyrin site with cellular reductants, must also be accounted for while designing or choosing the appropriate MnP, as experimental therapeutics in oxidative stress models.

Conclusions

Partition of isomeric Mn(III) *N*-alkylpyridylporphyrins between n-octanol and water, P_{OW}, was determined. The log P_{OW} is linearly related to thin-layer chromatographic parameter, R_f and to the number of carbon atoms with both *ortho* and *meta* isomers. Thus both parameters accurately describe drug lipophilicity. Yet, log P_{OW} may be more convenient and meaningful for the pharmaceutical and medical community particularly for the comparison of MnP to other drugs of similar therapeutic target that are in clinics or under development. The longer *ortho* *N*-alkylpyridylporphyrins, such MnTnHex-2-PyP and MnTnOct-2-PyP are significantly more lipophilic than MnTE-2-PyP and thus may be promising therapeutics, particularly in the cases of central nervous system injuries. Our data also show that *meta* isomers are 10-fold more lipophilic than *ortho* porphyrins and are in addition less bulky. Favorable lipophilicity and stericity would compensate for the lower antioxidant potency making meta isomers prospective antioxidants *in vivo* also.

Acknowledgments

IK, JSR, ZV and IBH acknowledge support from the National Institutes for Allergy and Infectious Diseases [U19AI067798], National Institute of Health [NIH R01 DA024074] and funding from The Wallace H. Coulter Translational Partners Grant Program; IS thanks NIH/NCI Duke Comprehensive Cancer Center Core Grant [5-P30-CA14236-29]. D.S. and I.B.H. thank for the support from NIH R01 DA024074. We are thankful to Irwin Fridovich for critically reading the manuscript.

Abbreviations Charges are omitted throughout text

MnP

Mn porphyrin

MnTalkyl-2

3-PyP^{5+} Mn(III) *meso*-tetrakis(*N*-alkylyridinium-2 or 3-yl)porphyrin, alkyl being methyl (M, AEOL10112), ethyl (E, AEOL10113), n-propyl (nPr), n-butyl (nBu), n-hexyl (nHex), n-heptyl (nHep), n-octyl (nOct)

2 and 3 relate to *ortho* and *meta* isomers

respectively

MnTDE-2-ImP^{5+}

Mn(III) tetrakis(*N*,*N*'-diethylimidazolium-2-yl)porphyrin, AEOL10150

MnTDMOE-2-ImP^{5+}

Mn(III) tetrakis[*N*,*N*'-di(2-methoxethyl)imidazolium-2-yl)porphyrin

P_{OW}

P_{OW}
: partition coefficient between n-octanol and water

P_{BW}
: partition coefficient between n-butanol and water

TLC
: thin-layer chromatography

$E_{1/2}$
: half-wave reduction potential

SOD
: superoxide dismutase

HIF-1α
: hypoxia inducible factor-1, NF-κB, nuclear factor κB

AP-1
: activator protein-1

References

1. Halliwell, B.; Gutteridge, JMC. Free Radical Biology and Medicine. Vol. 4. Biosciences; Oxford: 2007.
2. Van Empel VPM, Bertrand AT, Van Oort RJ, Van der Nagel R, Engelen M, Van Rijen HV, Doevendans PA, Crijns HJ, Ackerman SL, Sluiter W, De Windt LJ. EUK-8, a superoxide dismutase and catalase mimetic, reduces cardiac oxidative stress and ameliorates pressure overload-induced heart failure in the harlequin mouse mutant. J Am Coll Cardiol 2006;48:8245–832.
3. Salvemini D, Wang Z-Q, Zweier JL, Samouilov A, Macarthur H, Misko TP, Curie MG, Cuzzocrea S, Sikorski JA, Riley DP. A nonpeptidyl mimic of superoxide dismutase with therapeutic activity ion rats. Science 1999;286:304–306. [PubMed: 10514375]
4. Batinic-Haberle I, Benov L, Spasojevic I, Hambright P, Crumbliss AL, Fridovich I. The Relationship Between Redox Potentials, Proton Dissociation Constants of Pyrrolic Nitrogens, and *in Vitro* and *in Vivo* Superoxide Dismutase Activities of Manganese(III) and Iron(III) Cationic and Anionic Porphyrins. Inorg Chem 1999;38:4011–4022.
5. Goldstein S, Samuni A, Hideg K, Merenyi G. Structure-activity relationship of cyclic nitroxides as SOD mimics and scavengers of nitrogen dioxide and carbonate radicals. J Phys Chem A 2006;110:3679–3685. [PubMed: 16526651]
6. James AM, Cocheme HM, Smith RAJ, Murphy MP. Interactions of mitochondria-targeted and untargeted ubiquinones with the mitochondrial respiratory chain and reactive oxygen species. J Biol Chem 2005;28:21295–21312. [PubMed: 15788391]
7. Smith RAJ, Porteous CM, Ganes AM, Murphy MP. Delivery of bioactive molecules to mitochondria. Proc Natl Acad Sci 2003;100:5407–5412. [PubMed: 12697897]
8. Spasojevic I, Yumin C, Noel T, Yu I, Pole MP, Zhang L, Zhao Y, StClair DK, Batinic-Haberle I. Mn porphyrin-based SOD mimic, MnTE-2-PyP^{5+} targets mouse heart mitochondria. Free Radic Biol Med 2007;42:1193–1200. [PubMed: 17382200]
9. Batinic-Haberle I, Spasojevic I, Stevens RD, Hambright P, Fridovich I. Manganese(III) *Meso* Tetrakis *Ortho N*-alkylpyridylporphyrins. Synthesis, Characterization and Catalysis of $O_2^{\cdot-}$ Dismutation. J Chem Soc, Dalton Trans 2002:2689–2696.
10. Rebouças JS, DeFreitas-Silva G, Idemori YM, Spasojevic I, Benov L, Batinic-Haberle I. The impact of electrostatics in redox modulation of oxidative stress by Mn porphyrins. Protection of SOD-deficient *E. coli* via alternative mechanism where Mn porphyrin acts as a Mn-carrier. Free Radic Biol Med 2008;45:201–210. [PubMed: 18457677]
11. Ferrer-Sueta G, Vitturi D, Batinic-Haberle I, Fridovich I, Goldstein S, Czapski G, Radi R. eactions of Manganese Porphyrins with Peroxynitrite and Carbonate Radical Anion. J Biol Chem 2003;278:27432–27438. [PubMed: 12700236]

12. Zhao Y, Chaiswing L, Oberley TD, Batinic-Haberle I, StClair W, Epstein CJ, StClair D. A mechanism-based antioxidant approach for the reduction of skin carcinogenesis. Cancer Res 2005;65:1401–1405. [PubMed: 15735027]
13. Sheng H, Sakai H, Yang W, Fukuda S, Salahi M, Day BJ, Huang J, Paschen W, Batinic-Haberle I, Crapo JD, Pearlstein RD, Warner DS. Sustained treatment is required to produce long-term neuroprotective efficacy from a metalloporphyrin catalytic antioxidant in focal cerebral ischemia. Free Radic Biol Med. 2009submitted
14. Tse H, Milton MJ, Piganelli JD. Mechanistic analysis of the immunomodulatory effects of a catalytic antioxidant on antigen-presenting cells: Implication for their use in targeting oxidation/reduction reactions in innate immunity. Free Radic Biol Med 2004;36:233–47. [PubMed: 14744635]
15. Spasojevic I, Chen Y, Noel TJ, Fan P, Zhang L, Rebouças JS, StClair DK, Batinic-Haberle I. Pharmacokinetics of the potent redox modulating manganese porphyrin, MnTE-2-PyP^{5+} in plasma and major organs of B6C3F1 mice. Free Radic Biol Med 2008;45:943–949. [PubMed: 18598757]
16. Aslan M, Ryan TM, Adler B, Townes TM, Parks DA, Thompson JA, Tousson A, Gladwin MT, Tarpey MM, Patel RP, Batinic-Haberle I, White CR, Freeman BA. Oxygen Radical Inhibition of Nitric-Oxide Dependent Vascular Function in Sickle Cell Disease. Proc Natl Acad Sci USA 2001;98:15215–15220. [PubMed: 11752464]
17. Csont T, Viappiani S, Sawicka J, Slee S, Altarejos JY, Batinic-Haberle I, Schulz R. The Involvement of Superoxide and iNOS-Derived NO in Cardiac Dysfunction Induced by Pro-Inflammatory Cytokines. J Mol Cell Card 2005;39:833–840.
18. Cernanec JM, Weinberg BJ, Batinic-Haberle I, Guilak F, Fermor B. Oxygen tension modulates the effects of interleukin-1 on articular cartlidge matrix turnover via peroxynitrite. J Rheumatol 2007;34:401–407. [PubMed: 17295437]
19. Gauter-Fleckenstein B, Fleckenstein K, Owzar K, Jian C, Batinic-Haberle I, Vujaskovic Z. omparison of two Mn porphyrin-based mimics of superoxide-dismutase (SOD) in pulmonary radioprotection. Free Radic Biol Med 2008;44:982–989. [PubMed: 18082148]
20. Moeller BJ, Batinic-Haberle I, Spasojevic I, Rabbani ZN, Anscher MS, Vujaskovic Z, Dewhirst MW. A manganese porphyrin superoxide dismutase mimetic enhances tumor radioresponsiveness. Int J Rad Oncol Biol Phys 2005;63:545–552.
21. Moeller BJ, Cao Y, Li CY, Dewhirst MW. Radiation activates HIF-1 to regulate vascular radiosensitivity in tumors: Role of oxygenation, free radicals and stress granules. Cancer Cell 2004;5:429–441. [PubMed: 15144951]
22. Sheng H, Spasojevic I, Warner DS, Batinic-Haberle I. Mouse spinal cord compression injury is ameliorated by intrathecal manganese(III) porphyrin. Neurosci Lett 2004;366:220–225. [PubMed: 15276251]
23. Sompol P, Ittarat W, Tangpong J, Chen Y, Doubinskaia I, Mohammad Abdul H, Butterfield A, StClair DK. A neuronal model of Alzheimer's disease: An insight into the mechanisms of oxidative stress-mediated mitochondrial injury. Neuroscience 2008;153:120–130. [PubMed: 18353561]
24. Piganelli JD, Flores SC, Cruz C, Koepp J, Young R, Bradley B, Kachadourian R, Batinic-Haberle I, Haskins K. A Metalloporphyrin Superoxide Dismutase Mimetic (SOD Mimetic) Inhibits Autoimune Diabetes. Diabetes 2002;51:347–355. [PubMed: 11812741]
25. Sheng H, Enghild J, Bowler R, Patel M, Calvi CL, Batinic-Haberle I, Day BJ, Pearlstein RD, Crapo JD, Warner DS. Effects of Metalloporphyrin Catalytic Antioxidants in Experimental Brain Ischemia. Free Radic Biol Med 2002;33:947–961. [PubMed: 12361805]
26. Batinic-Haberle I, Ndengele MM, Cuzzocrea S, Rebouças JS, Spasojevic I, Salvemini D. Lipophilicity is a critical parameter that dominates the efficacy of metalloporphyrins in blocking morphine tolerance through peroxynitrite-mediated pathways. Free Radic Biol Med 2009;46:212–219. [PubMed: 18983908]
27. Okado-Matsumoto A, Batinic-Haberle I, Fridovich I. Complementation of SOD-deficient Escheria Coli by manganese porphyrin mimics of superoxide dismutase activity. Free Radic Biol Med 2004;37:401–10. [PubMed: 15223074]
28. Engelmann FM, Rocha SVO, Toma HE, Araki K, Baptista MS. Determination of n-octanol/water partition and membrane binding of cationic porphyrins. Int J of Pharm 2007;329:12–18. [PubMed: 16979860]

29. Batinic-Haberle I, Benov L, Spasojevic I, Fridovich I. The *Ortho* Effect Makes Manganese (III) *Meso*-Tetrakis(*N*-methylpyridinium-2-yl)Porphyrin (MnTM-2-PyP) a Powerful and Potentially Useful Superoxide Dismutase Mimic. J Biol Chem 1998;273:24521–24528. [PubMed: 9733746]
30. Rebouças JS, Spasojevic I, Batinic-Haberle I. Quality of Mn-porphyrin-based SOD mimics and peroxynitrite scavengers for preclinical mechanistic/therapeutic purposes. J Pharm Biomed Anal 2008;48:1046–1049. [PubMed: 18804338]
31. Lahaye D, Muthukumaran K, Hung C-H, Gryko D, Rebouças JS, Spasojevic I, Batinic-Haberle I, Lindsey JS. Design and synthesis of manganese porphyrins with tailored lipophilicity: Investigation of redox properties and Superoxide Dismutase activity. Bioorg Med Chem 2007;15:7066–7086. [PubMed: 17822908]
32. Thomas, G. Medicinal Chemistry: An Introduction. Vol. 2. John Wiley & Sons; West Sussex: 2007. p. 65-66.
33. Wagner RW, Johnson TE, Lindsey JS. Soluble Synthetic Multiporphyrin Arrays. 1. Modular Design and Synthesis. J Am Chem Soc 1996;118:11166–11180.
34. Hansch C, Leo A, Mekapati SB, Karup A. QSAR & ADMS. Bioorg Med Chem 3400;12:3391. [PubMed: 15158808]
35. Proudfoot JR. The evolution of synthetic oral drug properties. Bioorg Med Chem Lett 2005;15:1087–1090. [PubMed: 15686918]
36. Leo A, Hansch C, Elkins D. Partition coefficients and their uses. Chem Rev 1971;71:525–616.
37. Pollard J, Rebouças JS, Durazo A, Kos I, Gralla EB, Valentine JS, Batinic-Haberle I, Gatti RA. Radioprotective effects of manganese-containing superoxide dismutase mimics on ataxia telangiectasia cells. Free Radic Biol Med. 2008in press
38. Saba H, Batinic-Haberle I, Munusamy S, Mitchell T, Lichti C, Megyesi J, MacMillan-Crow LA. anganese porphyrin reduces renal injury and mitochondrial damage during ischemia/reperfusion. Free Radic Biol Med 2007;42:1571–1578. [PubMed: 17448904]
39. Batinic-Haberle I, Spasojevic I, Stevens RD, Hambright P, Neta P, Okado-Matsumoto A, Fridovich I. New Class of Potent Catalysts of $O_2^{\cdot-}$ Dismutation. Mn(III) methoxyethylpyridyl- and methoxyethylimidazolylporphyrins. J Chem Soc Dalton Trans 2004:1696–1702.
40. Rebouças JS, Spasojevic I, Tjahjono DH, Richaud A, Méndez F, Benov L, Batinic-Haberle I. Redox modulation of oxidative stress by Mn porphyrin-based therapeutics: The effect of charge distribution. Dalton Trans 2008:1233–1242. [PubMed: 18283384]
41. Batinic-Haberle I, Benov L, Spasojevic I, Fridovich I. The *Ortho* Effect Makes Manganese (III) *Meso*-Tetrakis(*N*-methylpyridinium-2-yl)Porphyrin (MnTM-2-PyP) a Powerful and Potentially Useful Superoxide Dismutase Mimic. J Biol Chem 1998;273:24521–24528. [PubMed: 9733746]
42. Wise-Faberowski L, Warner DS, Spasojevic I, Batinic-Haberle I. The effect of lipophilicity of Mn (III) *ortho N*-alkylpyridyl- and di*ortho N, N'*-imidazolylporphyrins in two *in-vitro* models of oxygen and glucose deprivation -induced neuronal death. Free Radic Res. 2008In press
43. Batinic-Haberle I, Spasojevic I, Stevens RD, Bondurant B, Okado-Matsumoto A, Fridovich I, Vujaskovic Z, Dewhirst MW. New PEG-ylated Mn(III) porphyrins approaching catalytic activity of SOD enzyme. Dalton Trans 2006:617–624. [PubMed: 16402149]
44. Spasojevic I, Batinic-Haberle I, Stevens RD, Hambright P, Thorpe AN, Grodkowski J, Neta P, Fridovich I. Manganese(III) biliverdin IX dimethyl ester: a powerful catalytic scavenger of superoxide employing the Mn(III)/Mn(IV) redox couple. Inorg Chem 2001;40:726–739. [PubMed: 11225116]

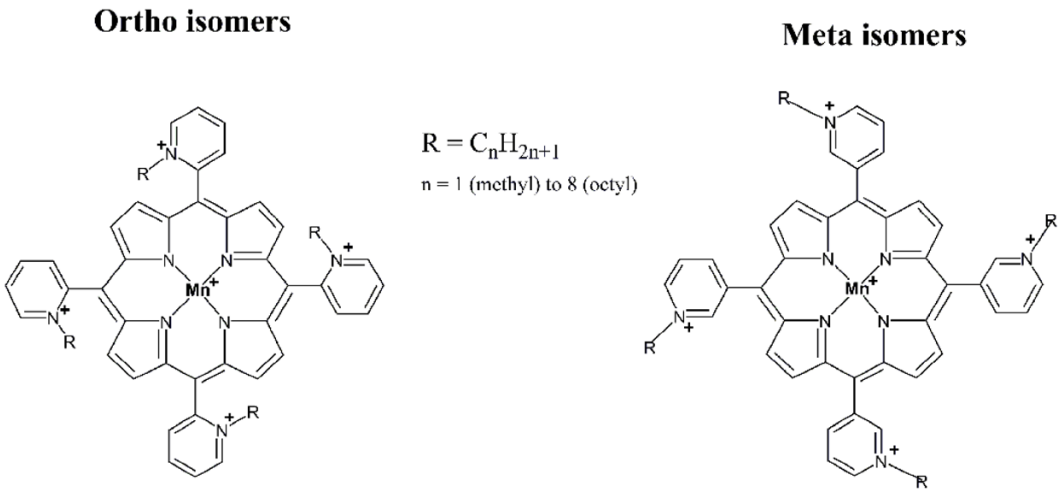

Figure 1.
Structures of *ortho* and *meta* isomers of Mn(III) *N*-alkylpyridylporphyrins.

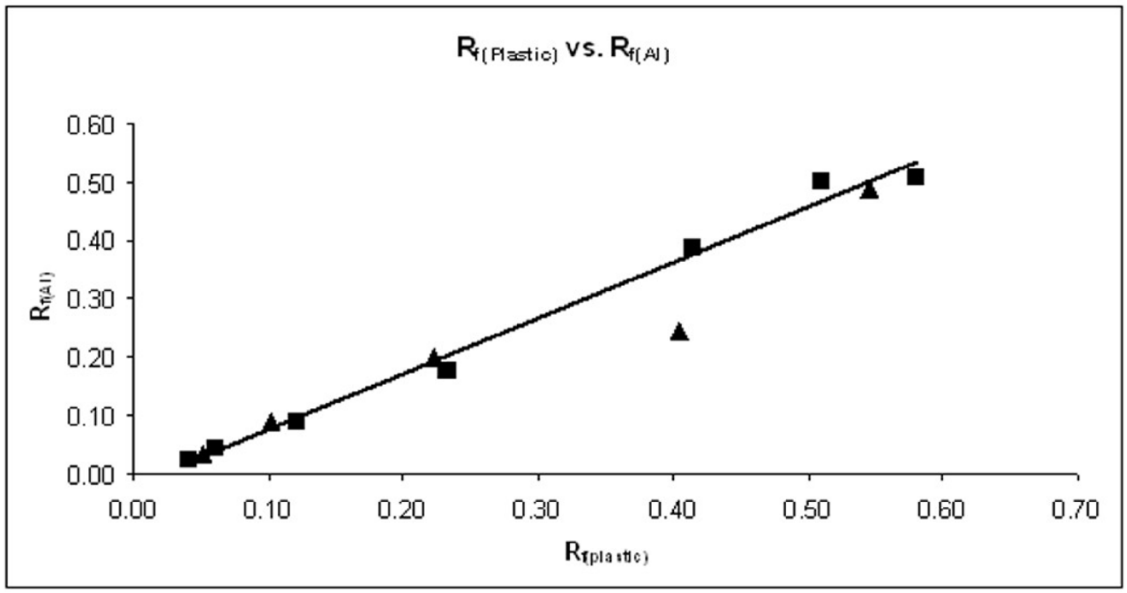

Figure 2.

The relationship between R_f obtained on TLC plastic-backed silica gel plates ($R_{f(Plastic)}$) and on TLC aluminum-backed silica gel plates ($R_{f(Al)}$) in acetonitrile: KNO_3-saturated H_2O:H_2O = 8:1:1. The *ortho* porphyrins are presented as squares (from methyl to octyl) and *meta* as triangles (from methyl to hexyl). The relationship is described with equation $R_{f(plastic)} = 0.91 \times R_{f(Al)} + 0.01$, $R^2 = 0.9609$.

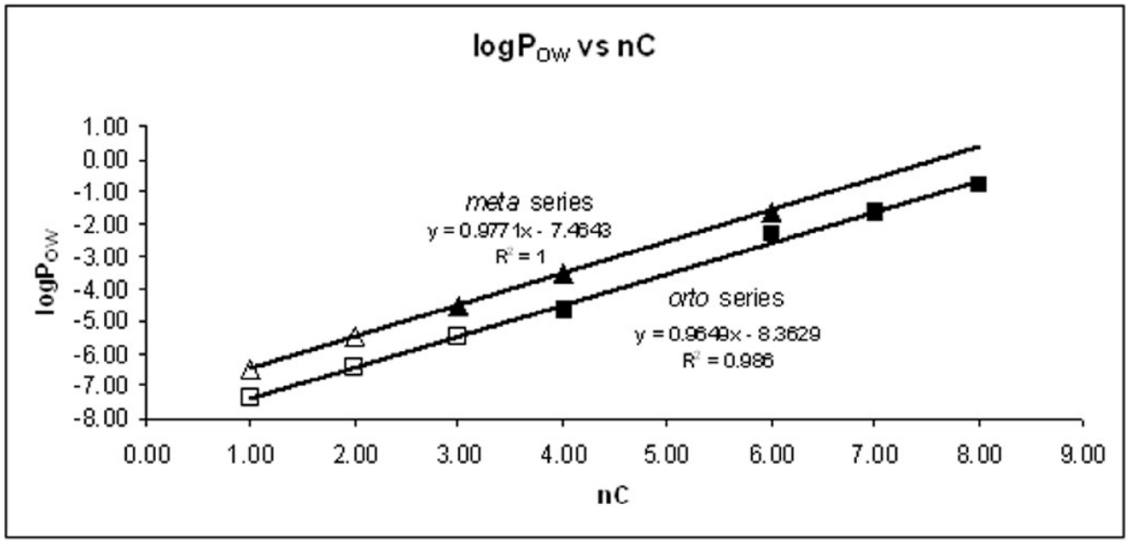

Figure 3.

Relationship between the log P_{OW} and the number of carbon atoms (nC) for the series of *ortho* and *meta* Mn(III) *N*-alkylpyridylporphyrins. Full squares (*ortho* isomers) and triangles (*meta* isomers) present experimental values (determined in water/n-butanol system and converted to water/n-octanol system using equation 2) while empty squares and triangles present predicted values, respectively. The porphyrins are from bottom to top: MnTM-2,3-PyP, MnTE-2,3-PyP, MnTPr-2,3-PyP, MnTnBu-2,3-PyP, MnTnHex-2,3-PyP, MnTnHep-2-PyP, MnTnOct-2,3-PyP.

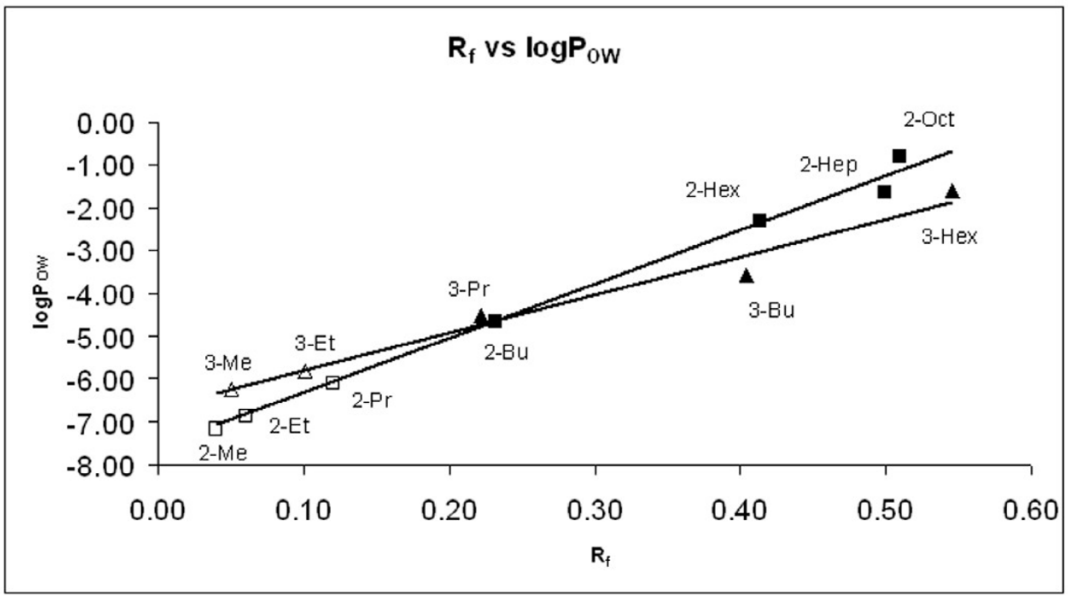

Figure 4.

Relationship between the thin-chromatographic parameter, R_f and log P_{OW} for the series of *ortho* and *meta* Mn(III) *N*-alkylpyridylporphyrins. R_f values refer to those calculated using plastic-backed TLC plates ($R_{f(Plastic)}$). Full squares (*ortho* isomers) and triangles (*meta* isomers) present experimental values (determined in n-butanol/water system and converted to n-octanol/water system using equation 2) while empty squares and triangles present predicted values, respectively. The porphyrins are from bottom to top: MnTM-2,3-PyP (2,3-Me), MnTE-2,3-PyP (2,3-Et), MnTPr-2,3-PyP (2,3-Pr), MnTnBu-2,3-PyP (2,3-Bu), MnTnHex-2,3-PyP (2,3-Hex), MnTnHep-2,3-PyP (2,3-Hep), MnTnOct-2,3-PyP (R_f value was determined on silica gel plates with plastic base in acetonitrile: KNO_3-saturated H_2O:H_2O = 8:1:1.) Equations for *ortho* series is log P_{OW} = 12.69 x R_f - 7.59 (R^2 = 0.9672) and for *meta* series is log P_{OW} = 8.89 x R_f - 6.70 (R^2 = 0.9316).

Table 1

Molar absorption coefficients of chloride salts of metal-free porphyrins and their Mn(III) complexes synthesized in this work. The data for other compounds can be found elsewhere [9,29][5] .

Porphyrin	λ_{max} (log ε^a)
H_2TnBu-3-PyP	810.0(2.72); 638.5 (3.09); 582.0 (3.85); 514.5 (4.28); 417.5(5.53); 262.5 (4.41)
H_2TnHex-3-PyP	830.0 (3.08); 823.0(3.05); 582.0 (3.76); 525.0 (4.20); 417.5 (5.43); 330.0 (4.28); 317.0 (4.25); 288.0 (4.08); 263.5 (4.34)
H_2TnHep-2-PyP	639.0 (3.47); 584.0 (3.86); 543.0 (3.65); 510.5 (4.27); 416.5 (5.34); 263.0 (4.36)
MnTnBu-3-PyP	843.0 (2.54); 830.0 (2.46); 786.0 (3.27); 675.0 (3.43); 558.0 (4.04); 502.5 (3.75); 460.0 (5.06); 396.0 (4.60); 373.5 (4.62); 262.0 (4.50)
MnTnHex-3-PyP	565.5 (3.29); 675.5 (3.18); 557 (4.03); 501.5 (3.75); 460.0 (5.06); 395.5 (4.57); 372.0 (4.59); 330.5 (4.43); 262.0 (4.45)
MnTnHep-2-PyP	779.5 (3.23); 559.5 (4.08); 502.5 (3.79); 454.0 (5.19); 414.5 (4.45); 364.5 (4.66); 261.5 (4.49)

[a]Molar absorption coefficient (M^{-1} cm^{-1}) were determined in water at room temperature (± 5%). λ_{max} (nm) were determined with errors within 0.5 nm.

Table 2

Electrospray ionization mass spectrometry of Mn(III) *N*-alkylpyridylporphyrins. Samples at 5 μM concentration were prepared in a H_2O-acetonitrile (1:1, v/v; containing 0.1 % v/v HFBA).

Peak Assignment	m/z					
	MnTnBu-3-PyPCl$_5$		MnTnHex-3-PyPCl$_5$		MnTnHep-2-PyPCl$_5$	
	Found	Calculated	Found	Calculated	Found	Calculated
[MnT(alkyl)-2,3-PyP^{5+} + 2HFBA$^-$]$^{3+}$/3	442.3,	442.1	479.7	479.7	498.4	498.2
[MnT(alkyl)-2,3-PyP^{5+} + HFBA$^-$2H$^+$]$^{2+}$/2	-	600.6	612.5	612.2	639.5	640.2
[MnT(alkyl)-2,3-PyP^{5+} + 2HFBA$^-$ - H$^+$]$^{2+}$/2	663.2,	662.6	-	718.7	746.8	746.7
[MnT(alkyl)-2,3-PyP^{5+} + 3HFBA$^-$]$^{2+}$/2	769.5	769.6	825.7	825.7	853.5	853.8

Table 3

The characterization of the lipophilicity and SOD-like activity of chloride salts of *ortho* and *meta* isomers of Mn(III) *N*-alkylpyridylporphyrins. R_f values refer to those calculated using plastic-backed TLC plates ($R_{f(Plastic)}$).

Porphyrin	R_f	log P_{OW} (determined)[a]	log P_{OW} (predicted)	log k_{cat}
MnTM-2-PyP	0.03		−7.40[c]	7.79
MnTE-2-PyP	0.06		−6.43[c]	7.76
MnTnPr-2-PyP	0.11		−5.47[c]	7.38
MnTnBut-2-PyP	0.19	−4.64		7.25
MnTnHex-2-PyP	0.38	−2.29		7.48
MnTnHep-2-PyP	0.46	−1.63		7.65
MnTnOct-2-PyP	0.49	−0.77		7.71
MnTM-3-PyP	0.05		−6.49[d]	6.61
MnTE-3-PyP	0.10		−5.41[d]	6.83
MnTnPr-3-PyP	0.22	−4.53		6.85
MnTnBut-3-PyP	0.40	−3.56		6.74
MnTnHex-3-PyP	0.55	−1.60		6.72

[a] $\log P_{BW}$ was determined experimentally using equation (1) and was converted to P_{OW} using equation (2);

[b] conditions: 0.05 M phosphate buffer, 0.1 mM EDTA, pH 7.8, 40 μM xanthine, ~ 2nM xanthine oxidase, 10 μM cytochrome *c*. The rate of cytchrome *c* reduction by $O_2^{\bullet-}$, $k_{cyt\ c} = 2.6 \times 10^5\ M^{-1}\ cm^{-1}$ is used for calculation of k_{cat} [44]. The estimated errors are within ±10 %.

[c] Calculated according to eq. (5).

[d] Calculated according to eq. (6).